CHEMISTRY OF MATERIALS

pubs.acs.org/cm

Article

Effect of Ring Mobility on the Dynamics of the Slide-Ring Gels

Sina Ghiassinejad,[+] Atul Kumar Sharma,[+] Charles-André Fustin,* and Evelyne van Ruymbeke*

Cite This: https://doi.org/10.1021/acs.chemmater.4c01235

Read Online

ACCESS | Metrics & More | Article Recommendations | Supporting Information

ABSTRACT: Random cross-linking in polymeric gels leads to heterogeneities in the obtained network, resulting in poor mechanical properties and limitations of practical applications. To overcome this issue, networks with movable cross-links have been developed. Slide-ring gels (SRGs), which are polymer networks with cross-links that can slide along the network strands, belong to this category. These gels are softer, more stretchable, tougher, and with good recovery properties due to the sliding of cross-links, which equalizes the applied stress on polymer strands. Although the origin of the excellent mechanical properties of these gels has been well-studied, the specific viscoelastic properties of slide-ring gels remain ambiguous due to the complexity of controlling and detecting the ring mobility. In this study, the development of a palladium-based slide-ring gel from a metal-coordinated pseudorotaxane motif enables us, for the first time, to control the ring's mobility without changing any other parameters and keeping the overall network connectivity. The rheology data of fixed-ring versus free-ring gels, analyzed with a tube-based model, reveal that the softness and lower elasticity of the slide-ring gels originate from the sliding of cross-links, which increases the effective mesh size of the network well above the length of a single polyrotaxane chain. Moreover, we demonstrate the key role played by the entanglements, which limit the sliding distance of the rings. This study thus provides new insights for understanding the peculiar viscoelastic behavior and huge stretchability of slide-ring gels, toward the rational design of SRGs with controlled properties.

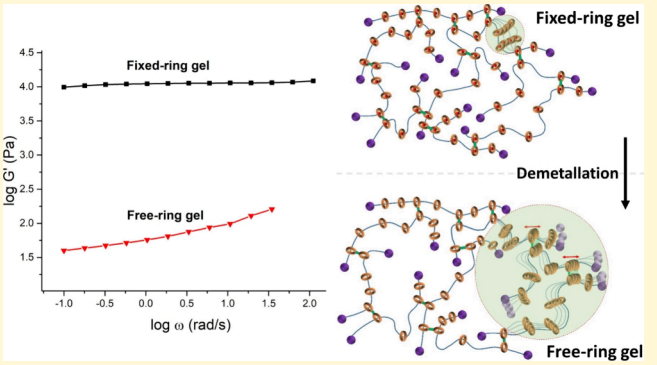

INTRODUCTION

Polymer gels, which are three-dimensional networks formed by chemically or physically cross-linked polymers containing a large amount of a solvent, offer considerable potential in, e.g., tissue engineering,[1] soft robotics,[2] sensors, actuators,[3,4] and drug delivery[5] applications. Their practical utility, however, is hindered by their low mechanical strength, often due to their uneven structure arising from an inhomogeneous cross-linking. To overcome this issue, networks with movable cross-links have been developed. Slide-ring gels (SRGs), which are polymer networks with cross-links that can slide along the network strands, belong to this category.[6,7] Their cross-link junctions are usually double rings forming a figure-of-eight shape, which are not fixed and can move freely to equalize tensions in the material in a manner similar to pulleys, which is thus called the "pulley effect".[7,8] Unlike the behavior of polymer chains in chemical gels, which gradually break under large deformation due to the heterogeneous polymer length between fixed cross-links,[9] the local mobility in slide-ring networks significantly influences the material properties leading to high stretchability,[10] self-healability,[11] adhesion,[12] and huge swellability.[13]

The most studied SRGs are based on polyrotaxanes made of α-cyclodextrin macrocycles (CDs) threaded on a poly(ethylene glycol) (PEG) chain.[6] Despite the fact that these SRGs suffer from the lack of an easy way to independently control important parameters such as ring−chain interaction and ring mobility,[14] many interesting properties have been highlighted with these systems. In particular, systematic research showed that the internal structure and properties of SRGs are highly dependent on the density of rings on the polymer axle.[15] For example, their huge stretchability is a clear outcome of the chain sliding through the cross-linked rings, which is favored at low ring densities.[7,14,16] Moreover, comparison between uniaxial tensile measurements on two slide-ring gels with a similar density of cross-linked rings but different densities of uncross-linked rings (single, free rings) showed that the extensibility of the gels decreases with an increasing density of uncross-linked rings. This was attributed to the fact that the uncross-linked rings create a counter pressure, which counteracts the sliding of the chains.[16] In all of these works, it is demonstrated that the increase of the sliding distance is the key point for developing the full potential of the

Received: April 27, 2024
Revised: August 10, 2024
Accepted: August 12, 2024

pulley effect. This effect has been further highlighted by Jiang et al., who synthesized an α-CD-based polyrotaxane with very low CD coverage (~2%), to obtain a gel with a sliding range of CD cross-links that is almost 65% of the length of the polymer axle.[17] The obtained gel was transparent and flexible and combined a high stress at break and a large extensibility of around 16 times its initial length. Later, the same group reported that under uniaxial stretching, the pulley effect allows the cross-links to slide on a large distance along the chains, leading to an inhomogeneous repartition of the cross-linked rings, with network strands much longer in the tensile direction than in the other directions, while preserving the complete recoverability of the sample.[18] This mechanism was also confirmed through molecular dynamics simulation (MD).[19] The influence of the ring size has also been investigated by comparing two similar SRGs made with CDs of different sizes. The results indicate that the gel with larger rings takes more time to relax due to the slower chain sliding through the larger rings. This effect was attributed to the increased interactions between the inner surface of larger CDs and the polymer chains.[20] It has been also reported that the formation of hydrogen bonds between the rings and chains can affect the ring mobility and consequently the rheological and mechanical properties of the slide-ring networks in the bulk[21] and gel states.[22] In the presence of H-bonds, the sliding motion of the rings along the polymer chains first requires to break the hydrogen bonds, which is an energy dissipation mechanism that improves the properties of the networks markedly.

In contrast to SRGs based on polyrotaxanes (PRs) and featuring figure-of-eight-shaped cross-links, the rotaxane cross-linked polymers (RCPs) are networks built from a (macromolecular) rotaxane cross-linker containing a single ring with the two reactive groups being located on the ring and at one end of the axle, respectively. This structure allows the ring to slide more freely along the rotaxane axle and facilitates the investigation of parameters affecting the ring−chain interactions, such as the ring size, axle thickness, and axle length.[23−25] In particular, with these materials, it has been shown that the toughness and fracture stress and strain are larger for the gels containing rotaxane cross-linkers (RCs) compared to typical covalent cross-linked polymers due to the ring mobility.[23] Tuning the axle thickness also influences the ring mobility, as thicker axles increase the molecular friction between the ring and the axle, and results in a lower stretchability of the network due to a lower ring mobility.[25]

To understand the impact of ring−chain interactions on the slidability of the rings and on the properties of slide-ring networks, all the studies reported above required the change of a network component such as the ring size[20] or axle thickness.[25,26] Currently, there is no example of a slide-ring network that allows a systematic study of ring−chain interaction without altering any other parameter of the network, particularly for polyrotaxane-based SRGs. The only reported work is about another kind of network architecture, made of doubly threaded slide-ring polycatenane networks.[27] In this very recent study, the authors used a small amount of metal-templated tetrafunctional pseudo[3]rotaxane (P3R) in a network made from 4-arm PEG stars. Each ring is thus threaded on two polymer chains, and it is the covalent cross-links that act as bulky "stoppers". Compared to an equivalent covalent gel with a similar gel fraction, the integration of metalated ring cross-links into the covalent network enhances the draining of the solvent when the sample is put under compression. Moreover, after demetalation of these networks, a notable decrease of the relaxation time of the gels was observed, speeding further the solvent draining. This result suggests that demetalated cross-linked rings are becoming mobile, which leads to a network with an adaptable mesh size, allowing the rings to slide and adjust to the network stress, thereby promoting faster solvent flow.

In the present work, we study how the ring mobility influences the viscoelastic properties of polyrotaxane-based slide-ring gels while keeping the other parameters and overall network connectivity constant. To this end, a palladium-based slide-ring gel is synthesized from a polyrotaxane, which is prepared from a palladium-templated pseudorotaxane motif.[28] Different research groups have exploited similar palladium-based 3 + 1 square planar complexes to prepare slide-ring networks,[26,29,30] but not based on polyrotaxanes, and the influence of demetalation, to modify the ring mobility, on the gel properties has not been investigated. Here, we investigate this effect in detail. Due to the presence of the metal−ligand complexes in the network, the ring mobility can be controlled by either keeping or removing the metal−ligand interactions between the ring and the axle. As shown in Figure 1, by using

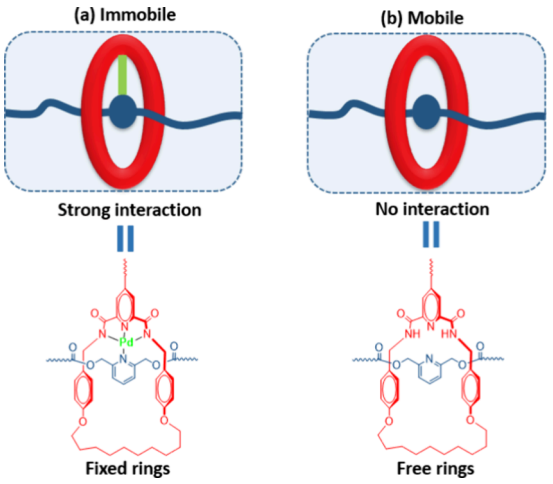

Figure 1. (a,b) Presentation of the two cases of ring mobility and ring−chain interaction in the slide-ring network developed in this work.

this palladium-based network, two different states of ring mobility, immobile (fixed) rings or free rings, can be achieved. Indeed, when the palladium is coordinated between the ring and the axle (Figure 1a), the network, if not largely deformed, essentially behaves like a covalent network due to the strong metal complexes holding the rings in place (fixed-ring gel). On the other hand, after demetalation, no interaction between the ring and the axle is present anymore, and the rings can move freely along the chains in the network (free-ring gel) (Figure 1b). Therefore, by comparing the dynamics of these gels, we gain insights into their viscoelastic behavior, structure, and stretchability.

Another objective of the present work is to take advantage of this well-defined SRG to investigate the origin of the low-frequency elastic plateau observed with SRGs.[31,32] When a constant deformation is applied to these gels, the latter is unable to fully relax the stress.[31,32] This remaining elasticity was attributed to the presence of numerous free (single) rings, which restrict sliding of the cross-linked rings. In the present

https://doi.org/10.1021/acs.chemmater.4c01235
Chem. Mater. XXXX, XXX, XXX−XXX

Scheme 1. Synthetic Route toward the Palladium-Based Polyrotaxane Network and Its Demetalation to Free the Rings

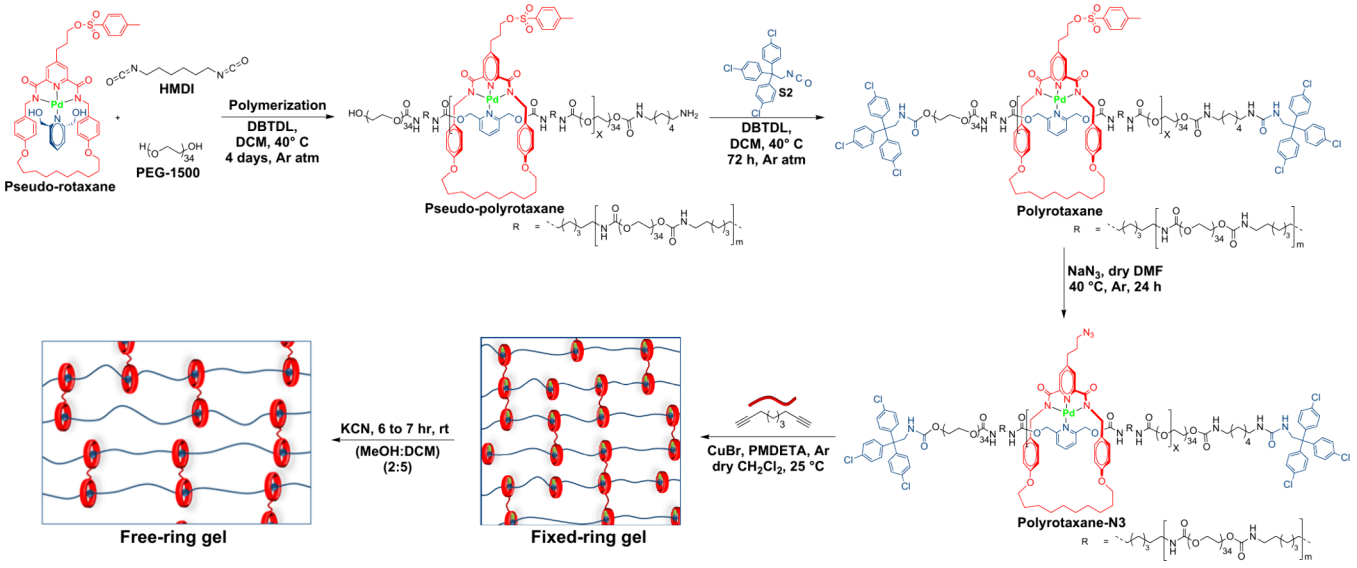

study, this explanation does not hold due to the limited presence of single rings. Therefore, with the help of a tube-based model, we analyze the viscoelastic properties of slide-ring gels to quantify the density of the cross-linked rings and propose a new molecular picture to explain the relationship between their composition and properties. Our results suggest that the softness and remaining elasticity found for the free-ring gel can be attributed to a combined effect of the low density of cross-links able to slide along the chain backbone, leading to an increasing mesh size with time and the presence of entanglements between the chain strands, which limits the sliding distance of the rings.

EXPERIMENTAL SECTION

Sample Characterization. ^{1}H NMR measurements were recorded on Bruker AVANCE 300 and 500 MHz FT-NMR spectrometers, and ^{13}C NMR spectra were recorded on Bruker 75 and 126 MHz FT-NMR spectrometers. All spectra were internally referenced to the solvent residual signals. The high-accuracy mass spectrometry analyses were performed on a Thermo Scientific Q Exactive mass spectrometer. The analyte solutions (1 mg/mL) were delivered to the ESI source by a Harvard Apparatus syringe pump at a flow rate of 9 μL/min. Typical ESI conditions were as follows: capillary voltage, 3.5 kV; cone voltage, 30 V; source temperature, 80 °C; desolvation temperature, 120 °C, capillary temperature, 320 °C. Size-exclusion chromatography (SEC) was carried out on a Agilent system composed of two PSS Gram columns (10 μm beads, porosity: 100 and 1000 Å) connected to an Agilent differential refractometer, with *N,N*-dimethylformamide containing 2.5 mM NH_4PF_6 as an eluent (35 °C, flow rate of 1 mL/min).

Rheology Measurements. The viscoelastic properties of all samples were investigated by small- and large-amplitude oscillatory shear rheology using an MCR 301 (Anton Paar, Germany) rheometer. The temperature was controlled using a convection oven operating under nitrogen for measuring within the temperature range of 90−40 °C. For the gel samples, a solvent trap was designed to be used with the Peltier plate cooling system. In this Peltier cooling system, the cooling/heating medium was an antifreeze liquid, which circulated in the Peltier in order to regulate the temperature of the lower plate of the rheometer. Such a system allows varying the temperature of measurements from −50 to 220 °C. A parallel-plate geometry (diameter of 8 mm) was used as the upper plate. During the measurements, no slip problem was observed due to the good adhesion of the polymers and gels to the surface of the steel geometry. On the other hand, the reproducibility of the rheological measurements with different gaps was checked for each sample to confirm the absence of the slippage during the measurements. The melt sample was loaded at 50 °C and stabilized for 30 min, while for the gels, a temperature of 25 °C was used during 20 min. It should be mentioned that loading the gels within the rheometer is a bit tricky as we should be careful to avoid breaking the network by squeezing it under the spindle. For each sample, consecutive frequency sweeps were performed, at temperatures separated by steps of 10 °C, for the different samples. For checking the reproducibility of the measurements, all measurement was performed twice, from low to high temperatures and vice versa. The data were always found to be the same.

RESULTS AND DISCUSSION

Synthesis of Slide-Ring Gels. The polyrotaxane and the slide-ring gels were synthesized following our previously reported procedure.[28] Briefly, a polyrotaxane was first synthesized in two steps. To this aim, the pseudorotaxane (0.4 equiv), PEG-1500 (0.6 equiv), and hexamethylene diisocyanate (1 equiv) (HMDI) were reacted together in the presence of a catalytic amount of dibutyl tin dilaureate (DBTDL) at 40 °C in dry dichloromethane (DCM) under an inert atmosphere to obtain a pseudopolyrotaxane as shown in Scheme 1. After the desired reaction time, the reaction was quenched with a 2:8 mixture of water and acetone to convert all the remaining isocyanate functional groups into primary amines. The quenched pseudopolyrotaxane was then isolated and dried to further react with the isocyanate-functionalized **S2** bulky stopper to produce the desired polyrotaxane. The next step was the cross-linking of the polyrotaxane by linking the macrocycles two-by-two to form a three-dimensional network. To this end, the tosyl group on the macrocycles was first substituted by an azide, and the cross-linking was then performed by the copper(I)-catalyzed alkyne−azide cyclo-addition (CuAAC) "click" reaction using a dialkyne cross-linker. The gel was finally washed with an EDTA solution to remove the copper ions and rinsed with water then methanol and finally DCM, before being dried in air for at least 48 h (see the Supporting Information for details).

The removal of the palladium ions was performed by adding KCN, a strong competitive ligand, since this is an efficient

https://doi.org/10.1021/acs.chemmater.4c01235
Chem. Mater. XXXX, XXX, XXX−XXX

Table 1. Composition of the Polyrotaxane Used to Prepare the Slide-Ring Gels

							avg. no. of rings per chain	
sample name	code	ratio PEG:ring	M_n(g/mol)(SEC)	M_w(g/mol)(SEC)	$Đ$	M_n(g/mol) (^{1}H NMR)	SEC	^{1}H NMR
polyrotaxane	PR41k	0.6:0.4	21,000	41,000	1.97	26,000	5.6	6.5

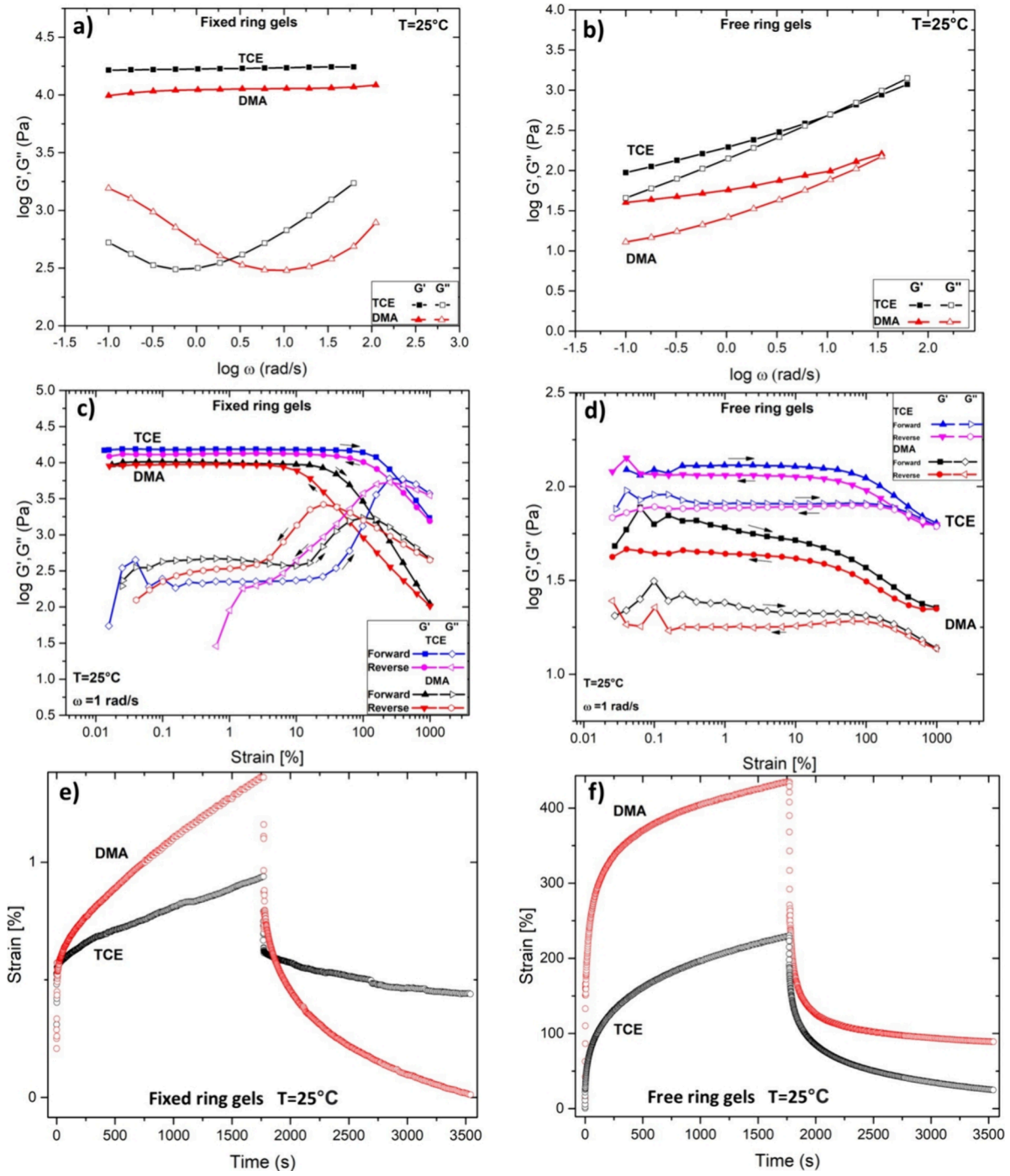

Figure 2. Viscoelastic behaviors of gels swollen in DMA or TCE (35 wt %/v). Storage and loss modulus as a function of the angular frequency for (a) fixed-ring gels and (b) free-ring gels. Amplitude sweep measurements of (c) fixed- and (d) free-ring gels. Creep-recovery measurements for the (e) fixed- and (f) free-ring gels.

method as previously reported in different works based on this 3 + 1 palladium chemistry.[33−36] As shown in Scheme 1, the palladium was removed by treating the gel with KCN in a 2:5 mixture of MeOH/DCM at room temperature for 6 to 7 h. After demetalation, the gel was washed with methanol and dried in air for at least 48 h. Table 1 shows the detailed information on all samples, which have been used in this paper. The dried metal-containing and demetalated gels were finally

https://doi.org/10.1021/acs.chemmater.4c01235
Chem. Mater. XXXX, XXX, XXX−XXX

swollen again for 24 h in the targeted final solvents at a polymer concentration of 35 wt %/v. Two solvents with a high boiling point, to be compatible with the rheology measurements, and of opposite polarity were selected to study ring mobility in different environments. *N*,*N*-Dimethylacetamide (DMA) was chosen as a polar solvent and 1,1,2,2-tetrachloroethane (TCE) as a nonpolar solvent. All gels were intact despite the rather large swelling ratio due to the presence of the stoppers, which prevent the unthreading of the rings.

The polyrotaxane samples were analyzed by SEC and ^{1}H NMR (Table 1). The molar mass dispersity of the polyrotaxane is close to 2, as expected for a polyaddition polymerization. The molar mass of the polyrotaxane was obtained by both SEC with PEG standards and ^{1}H NMR by comparing signals of the protons of the stoppers at the chain ends with the signals of the polymer main chain (PEG, urethane spacer). As seen in Table 1, both methods give values in good agreement.

The ratio between PEG/HMDI and macrocycle/HMDI can be established from the ^{1}H NMR spectra (see the Supporting Information for details). The ratio of PEG/HMDI was found to be 0.59, while the macrocycle/HMDI ratio was 0.38, very close to the feed ratio values of 0.6 and 0.4 respectively. This shows that our synthesis approach enables control of the average number of rings per polyrotaxane. Finally, the average number of macrocycles per polyrotaxane chain was determined both from ^{1}H NMR, by comparing the signals of the stoppers to the signals of the macrocycles, and from the SEC molar mass, knowing the ratio between PEG, macrocycle, and HMDI. Both methods gave a similar value of around 6 macrocycles per chain (see Table 1).

Viscoelastic Properties of the Slide-Ring Gels. The effect of the ring mobility on the dynamics of slide-ring gels is investigated based on their shear viscoelastic properties, both in the linear and nonlinear regimes of deformation (details on the measurements are given in the SI) and in both DMA and TCE. We first performed dynamic oscillatory shear measurements. Figure 2a,b presents the storage and loss moduli of the fixed- and free-ring gels, as a function of the frequency with an amplitude of deformation fixed to 1%, to ensure that the data are in the linear regime. In both solvents, the fixed-ring gel shows a clear rubbery plateau of around 10 kPa, which is frequency-independent, as expected for a polymer network formed by strong interactions. On the other hand, the free-ring gels have a much weaker elastic response. A lower elastic contribution in the free-ring gel was expected since after removing the Pd ions, the rings are expected to be able to slide along the polymer strands, which leads to their partial relaxation. However, such a huge drop of G' was not foreseen. The origin of this large drop is investigated in the modeling section. Briefly, it is attributed to the very low average number of rings per chain, leading to a low cross-link density and a large sliding distance of the rings.

Furthermore, as mentioned in the Introduction, it has been shown in the literature that SRGs usually show two elastic plateaus.[31,32,37,38] The transition from the high rubbery plateau at a high frequency (short time) to the low elastic plateau at a low frequency (long time) has been attributed by Ito et al. to a reptation-like local diffusion of the chains through the cross-linked rings.[31,32] This transition is thus a consequence of the partial sliding of the chain segments through the movable cross-links, which leads to partial relaxation of the network. Another possible explanation has been given by Fleury et al., who proposed that the transition regime is due to the fluctuation of the mean mass distribution between the cross-link points due to sliding of the axle through the rings.[37] This process leads to a gradual increase of the effective mesh size and consequently to a decrease of the storage modulus. The lower frequency plateau, indicating that the gel is unable to fully relax, was attributed by Ito and Kato[31] to a heterogeneous distribution of the free CD rings generated by the deformation that creates a new type of entropic elasticity, called sliding elasticity.

In the present work, it is observed that the storage modulus of the free-ring gel does not show two elastic plateaus. It first decreases from a high to intermediate frequency before eventually reaching a plateau, or at least the beginning of a plateau, at a lower frequency. As this plateau is much lower than that found with the fixed-ring gel, we attribute it to the remaining sample elasticity after the partial relaxation of the movable network strands. Its presence suggests that a part of the network strands is unable to relax despite the mobility of the free cross-linked rings. However, contrary to the usual SRGs made of CDs threaded on PEG, the remaining elasticity cannot be attributed to the sliding elasticity induced by the motion of the free rings since in our case, the density of rings is very low. The possible origin of this remaining elasticity is further explored in the modeling section.

To investigate the possible role of the solvent polarity in the ring mobility, the viscoelastic properties of the fixed-ring and free-ring gels have been investigated with two different solvents, TCE and DMA. When swollen in TCE, a nonpolar solvent, hydrogen bonds are expected between polymer threads through the urethane moieties and possibly also between the rings (containing two amides and a pyridine; see Figure 1b) and the polymer axle for the free-ring gel. Former works have shown that the presence of H-bonds in materials with movable cross-links can lead to an increase in the mechanical and viscoelastic properties.[21,22] On the other hand, these interactions should be mostly absent in DMA, which is a good H-bond acceptor. The viscoelastic properties of the fixed-ring and free-ring gels in both solvents are compared in Figure 2a,b. In addition to having slightly higher moduli, the gels in TCE have segmental dynamics that is slowed down (for the fixed-ring gels, this delay can be seen on the loss modulus data). As shown in Figure S6, the same delay is found for the viscoelastic properties of the reference polyrotaxane sample, before its cross-linking. This delay is further quantified in the modeling section, where it is seen that in TCE, the chain dynamics is slowed down by a factor of around 20 compared to the dynamics of the sample in DMA. This suggests that, while H-bonds may exist, they do not affect the overall softness of the SRGs. Their only effect is to slow down the time that the chain strands and polyrotaxane need to move and explore their surroundings to partially relax their stress when a deformation is applied.

To investigate the nonlinear properties of the networks and their ability to resist large deformations, amplitude sweep tests have been performed at room temperature (at an angular frequency of ω = 1 rad/s). First, the deformation amplitude was increased from 0.01 to 1000% followed by the reverse test, from 1000 to 0.01% (Figure 2c,d). At low amplitudes of deformation, the storage and loss moduli of fixed-ring gels are higher than for the free-ring gels, in agreement with the frequency sweep data. With increasing the deformation amplitude, a crossover between G' and G'' is observed (Figure

https://doi.org/10.1021/acs.chemmater.4c01235
Chem. Mater. XXXX, XXX, XXX−XXX

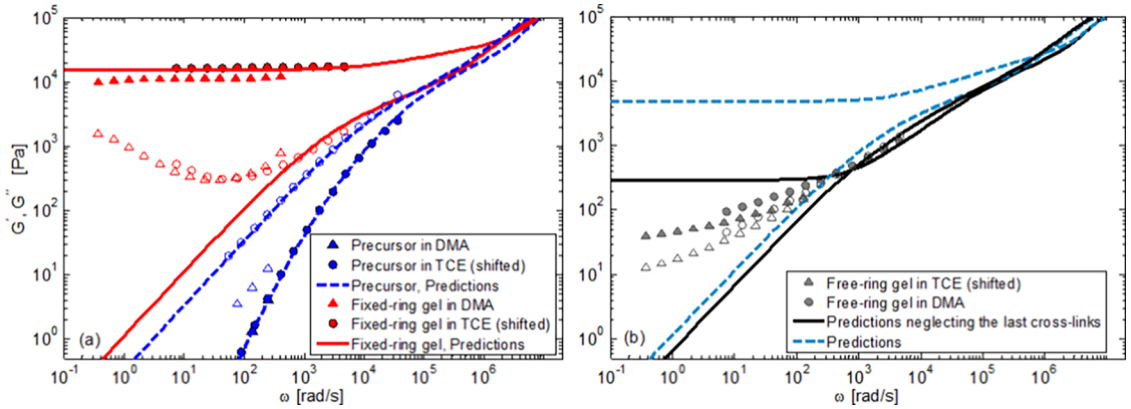

Figure 3. (a) Storage and loss moduli as a function of the angular frequency of the polyrotaxane precursor and of the fixed-ring gels. The data in TCE (circles) have been shifted horizontally to the high frequency by a factor of 20 to superimpose with the data in DMA (triangles). The data are compared to the theoretical curves, with M_{xx} = 23kg/mol (continuous curves). (b) Storage and loss moduli as a function of the angular frequency of the free-ring gel. The data in the TCE (circles) have been shifted horizontally to the high frequency by a factor 20 to superimpose with the data in the DMA (triangles). The theoretical curves have been obtained by assuming that the free rings do not contribute to the long-term elasticity, without (dashed curves) or with (continuous curves), allowing CLFs to occur down to the second-outer-ring cross-links.

2c), above which the fixed-ring gels display a liquid-like response (with $G' < G''$), which suggests that the network is partially broken under large deformations. However, even at 1000% deformation, their storage modulus stays larger than the storage modulus of the free-ring gels at equilibrium (Figure 2d), suggesting that even under large deformations, the fixed-ring gels still contain a certain fraction of fixed cross-links. Since these samples are very sticky, slippage is improbable. Interestingly, when the amplitude of deformation is decreased, the fixed-ring gels show a hysteresis and recover their initial viscoelastic properties. This indicates that the observed alteration of the network is reversible (as also shown by the frequency sweep tests in Figure S7a,b). Therefore, we attribute this effect to the dissociation of the palladium complexes between the ring and thread, which is triggered by the large deformation imposed. These metal−ligand interactions can progressively reform at low deformation, which explains the hysteresis between the two curves. This result is in agreement with recent findings of Yan's group who reported on mechanically interlocked networks where the ring of a [2]rotaxane motif was able to move back quickly to its initial ammonium binding site after being pulled away by a large deformation.[39]

On the other hand, the free-ring gels in both solvents do not break even under a 1000% strain, at which the crossover between G' and G'' is not yet reached. The large resistance to rupture of the free-ring gels is attributed to the mobility of the cross-links. Since the rings can move along the polymer chain, the sample can better adapt to the deformation and equalize the tension, which helps prevent stress concentration and retards sample breaking. The continuous, gradual decrease in the storage modulus of the free-ring gel in DMA can be attributed to the ceaseless fluctuation of axle segments through movable cross-links under deformation. This leads to the creation of a looser and shear-resistant network.[39] This phenomenon is less pronounced in the presence of H-bonds in TCE. When the amplitude of deformation is decreased in the reverse cycle, the initial level of the moduli is almost recovered. Its slightly lower level (see also G' and G'' measured after the strain sweep tests in Figure S7c,d) is attributed to few irreversible changes (such as the unthreading of few macrocycles or the breaking of a few chains) at these high deformations. As for the frequency sweep tests, the main effect of possible secondary interactions induced by the use of TCE is a slightly higher elasticity of the gels (Figure 2c,d). However, interestingly, the deformation amplitude at which the fixed-ring gel enters the nonlinear regime is larger in TCE than in DMA, despite its higher modulus. This result suggests that the secondary interactions increase the toughness of the gels, as already observed with sliding-ring networks containing secondary transient cross-links.[40]

Finally, creep-recovery measurements are presented in Figure 2e,f to discuss the extensibility of the samples and their elastic memory. The temperature was fixed to 25 °C, and the samples were deformed under a constant stress of 50.7 Pa (the torque is 5 μN m) for 1800 s. While the fixed-ring gels are nearly not deformed (less than 2% deformation), the free-ring gels under the same conditions reach a high level of deformation in both DMA and TCE, of almost 400 and 250%, respectively, while being able to recover more than 80% of their initial shape when removing the stress (Figure 2f and Figure S8). This result highlights the fact that the movable cross-links allow us to obtain polymer gels with a large deformability while preserving the coherence of the network. The gels in TCE are less deformable than those in DMA, which is attributed to the presence of secondary interactions that strengthen the network.

Modeling the Viscoelastic Properties of the Slide-Ring Gels. To further understand the dynamics of the slide-ring gels, we analyze their linear viscoelastic data with the help of a tube-based model. To this end, we first look at the viscoelastic properties of the polyrotaxane (PR41k) precursor in both DMA and TCE. As already mentioned, the PR sample diluted in TCE relaxes around 20 times slower than that in DMA (Figure S6). The same delay is observed with the fixed-ring gels and the free-ring gels in the two solvents (Figure 2) and can be attributed to the presence of H-bonds, which increase the interchain friction and therefore delay the segmental dynamics. If we account for this delay by horizontally shifting the data in TCE toward higher frequencies, then the viscoelastic curves in both solvents superimpose rather well (Figure 3), suggesting that the solvent nature does not affect the density of entanglements and cross-links present in the gel. Indeed, such an effect would have

https://doi.org/10.1021/acs.chemmater.4c01235
Chem. Mater. XXXX, XXX, XXX−XXX

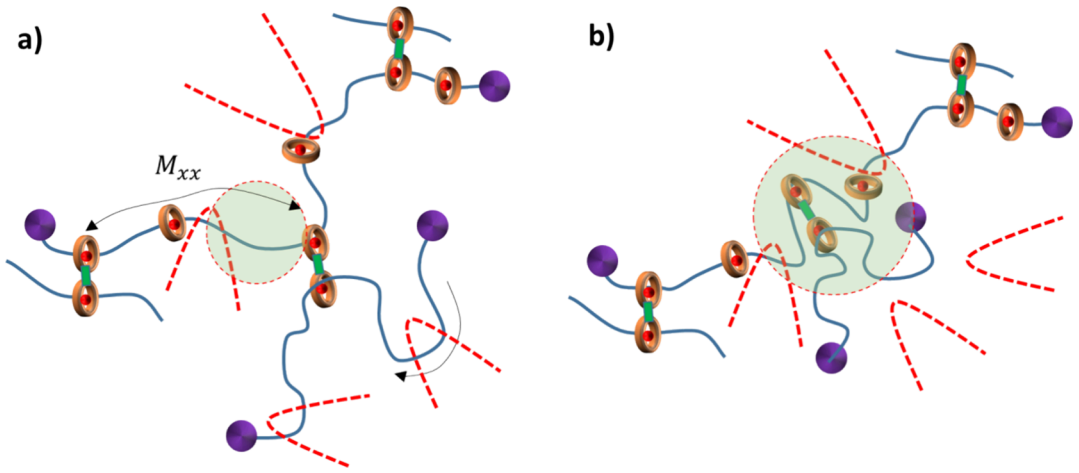

Figure 4. (a) Schematic drawing of the fixed-ring gel. The mesh size, represented by the green circle, determines the level of the elastic plateau. It accounts for both the entanglements (dashed red curves) and ring cross-links. (b) For a long time, the fixed-ring cross-links threaded by a chain containing only one ring cross-link cannot be considered as a topological constraining point. This leads to the slow relaxation of longer network strands (represented by the green circle).

influenced the level of the storage modulus, which is not observed.

The time marching algorithm (TMA) tube model is then used to describe the viscoelastic properties of the PR precursor. As the chains have an average molar mass in weight of 41 kg/mol, we must account for the possible presence of interchain entanglements. This model has been explained in details in refs 41 and 42. Here, we just report the main equation of the relaxation modulus $G(t)$:

$$G(t) = G_{\text{Rouse}}(t) + G_N^0 \varphi(t) \phi_{\text{tube}}(t) \quad (1)$$

where G_N^0 is the plateau modulus, $\varphi(t)$ is the weight fraction of the entanglement strands, which are not yet relaxed by tube escaping mechanisms such as reptation and contour length fluctuations, and $\phi_{\text{tube}}(t)$ is the dilation factor, which accounts for the influence of the relaxation of the surrounding chains on the probe chain. In the case presented here, this factor is well-approximated by $\phi_{\text{tube}}(t) = \varphi(t)$. The function $G_{\text{Rouse}}(t)$ describes the local relaxation of the entanglement segments by a Rouse process as well as the effect of its longitudinal modes along the tube:

$$G_{\text{Rouse}}(t) = \sum_i v_i \frac{\rho RT}{M_i} \left[\sum_{p=Z_i+1}^{N} \exp\left(-\frac{2p^2 t}{\tau_R(M_i)}\right) + \frac{1}{4} \sum_{p=1+1}^{Z_i} \exp\left(-\frac{p^2 t}{\tau_R(M_i)}\right) \right] \quad (2)$$

with v_i, M_i, Z_i, and $\tau_R(M_i)$ being the weight fraction, the molar mass, the number of entanglements, and the Rouse time of the chains i. ρ is the density of the PEO chains diluted at 35 wt %/v (taken here as equal to 0.4 g cm^{-3}), R is the gas constant, and T is the temperature. This model is based on two material parameters: the molar mass between two entanglements, M_e, and the proportionality factor K_{Rouse} of the Rouse relaxation time of a molecular segment, $\tau_R(M) = K_{\text{Rouse}} M^2$. To obtain good agreement with the viscoelastic response of the diluted precursor, K_{Rouse} in DMA has been fixed to 2×10^{-15}, while its value is 20 times larger in TCE. Moreover, in both solvents, the molar mass between two entanglements, M_e, has been fixed to 11,500 g/mol, which corresponds to $G_N^0 = \frac{4}{5}\frac{\rho RT}{M_e}$=90 kPa The value of M_e is higher than the value expected for pure PEO chains diluted at 35 wt %/v, which is around 7000 g/mol.[43] This is attributed to the fact that the chain backbone is not made of pure PEO but contains many other moieties. It is seen in Figure 3a that the model accurately describes the data (see the blue curves). No clear rubbery plateau is observed due to the low number of entanglement segments per chains (in average, $Z = \frac{M_w}{M_e} = 3.56$).

Viscoelastic Properties of the Fixed-Ring Gels. Based on these parameters, we then model the viscoelastic properties of the corresponding fixed-ring gels. To this end, assuming that the average molar mass M_{xx} between two fixed-ring cross-links is known (Figure 4a), we randomly locate these cross-links along the backbones of a large ensemble of chains, which have been chosen to represent the experimental molar mass distribution. The probability of a monomer of molar mass m_0 to be a fixed-ring cross-link is equal to $(M_{xx}/m_0)^{-1}$. Following ref 44, the chain sections are then classified into different categories. The linear chains (without cross-links) and the dangling arms, located close to the chain extremities, can disentangle and relax. On the other hand, chain sections trapped between two cross-links are unable to diffuse and disentangle. The latter chain sections can only partially relax thanks to the motion of the surrounding chains via the constraint release process, which is taken into account by the dilation factor $\phi_{\text{tube}}(t)$.[44]

Their restricted motion gives rise to a permanent elastic plateau observed in the storage modulus data, and the corresponding relaxation modulus $G(t)$ of the fixed-ring gel is defined as

$$G_{\text{fixed ring}}(t) = G_{\text{Rouse}}(t) + G_N^0 \varphi_{\text{fixed ring}}(t) \phi_{\text{tube}}(t) + \frac{\rho RT}{M_{xx}} v_{\text{trapped}} \quad (3)$$

with $\varphi_{\text{fixed ring}}(t)$, the fraction of chain segments, which are not relaxed at time t. It is defined as

$$\varphi_{\text{fixed ring}}(t) = v_{\text{trapped}} + \sum_{i,\text{dangling}} v_{i,\text{dangling}} \varphi_{i,\text{dangling}}(t) \quad (4)$$

https://doi.org/10.1021/acs.chemmater.4c01235
Chem. Mater. XXXX, XXX, XXX−XXX

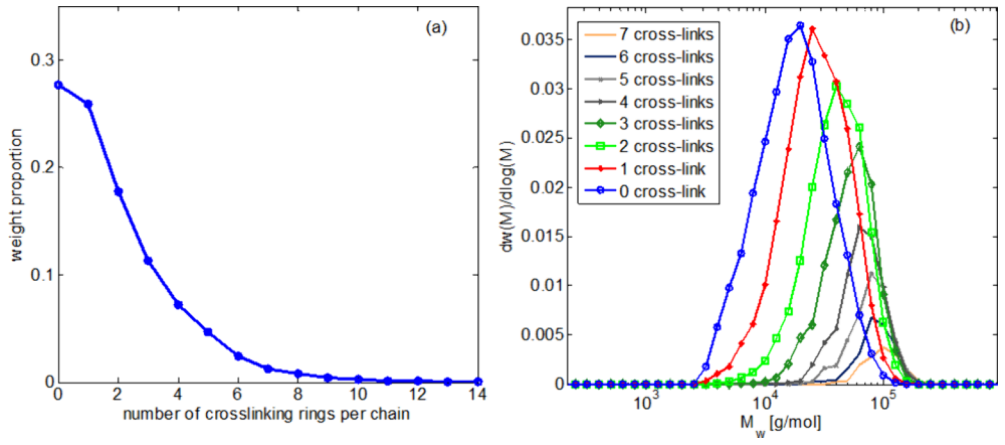

Figure 5. (a) Weight fraction of chains as a function of their number of ring cross-links, assuming that M_{xx} = 23 kg/mol. (b) Molar mass distribution of the chains containing a certain number of ring cross-links (see the legend).

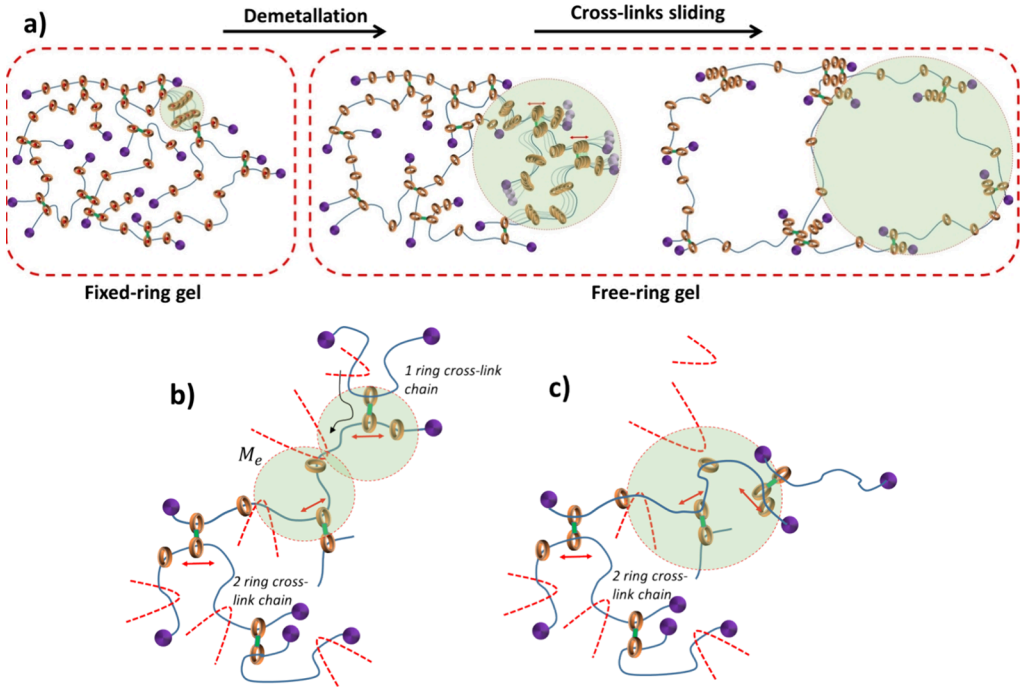

Figure 6. (a) Schematic image of the proposed mechanism for the relaxation of slide-ring gels while neglecting the effect of entanglements. With time, the length of the network strands, which are able to relax, increases thanks to the ability of the strands to slide through the rings. This leads to the increase in the effective mesh size (represented by the green circle). (b) Accounting for the entanglements, we consider that once the ring cross-links can slide, the mesh size is equal to the entanglement segments. (c) Due to the low number of ring cross-links per chain, there is a large probability that the entanglements located close to the chain extremities can relax.

where $\upsilon_{\text{trapped}}$ is the total weight fraction of chain segments trapped between two ring cross-links, unable to relax. On the contrary, the dangling chain segments are able to disentangle and therefore do not contribute to the long-term elasticity (see Figure 4). The parameters $\upsilon_{i,\text{dangling}}$ and $\varphi_{i,\text{dangling}}$ are the weight fraction and the survival probability of dangling and linear chains of mass M_i. The dilation factor $\phi_{\text{tube}}(t)$ is approximated well by $\phi_{\text{tube}}(t) = \varphi_{\text{fixed ring}}(t)$. In eq 3, the last term accounts for the influence of the additional cross-link junctions on the plateau modulus. As shown in Figure 3a, a good description of the data is obtained if we consider M_{xx} = 23 kg/mol. The latter value means that, on average, the chains only contain around two fixed rings, which act effectively as interchain cross-links. We attribute this low number, compared to the theoretical value of 6 rings per chain, to network defects like uncross-linked rings or primary loops in the sample that cannot be considered as effective cross-linked rings in the model. From this analysis, we conclude that in this gel, the density of entanglements (M_e = 11.5 kg/mol) is larger than the density of effective ring cross-links (M_{xx} = 23 kg/mol). The remaining elasticity of the network is thus largely due to the entanglements between network strands, which are unable to relax since they are trapped between two ring cross-links (Figure 4a).

The corresponding weight fractions of chains containing a fixed number of effective ring cross-links are shown in Figure 5a. It has been determined statistically based on the experimental molar mass distribution and on the probability for a monomer to be an effective ring cross-link. It is observed that around 70 wt % of the chains contain only 0, 1, or 2 cross-

https://doi.org/10.1021/acs.chemmater.4c01235
Chem. Mater. XXXX, XXX, XXX−XXX

linked rings, which effectively participate to the network. As shown in Figure 5b, only the longer chains may contain a larger number of cross-links. However, this number remains rather low.

On Figure 3a, it is also observed that a small fraction of the fixed-ring gel is going to relax at a low frequency (below 0.1 rad/s). This relaxation process, which has a little effect on the storage modulus, is more visible on the loss modulus, which increases at a lower frequency. We attribute it to the influence of the chains containing only one ring cross-link. Indeed, as illustrated in Figure 4b, these chains can disentangle and relax. While this effect is taken into account in eq 3, we should also consider that their motion may allow the corresponding ring cross-link to move and, consequently, to not act as cross-linking point anymore. In such a case, the effective mesh size of the network is further increased (see the green circle in Figure 4b). Since this slow relaxation process is not taken into account in the model, a large discrepancy between the experimental and predicted G'' curves is observed at a low frequency.

Viscoelastic Properties of the Free-Ring Gels. We can now use this distribution of fixed-ring cross-links to further investigate the viscoelastic properties of the slide-ring gels. In this case, the only difference is that the rings are able to slide along the chain backbone. As observed in Figure 3b, the elastic plateau of the free-ring gels is very low compared to that of the fixed-ring gels. To understand this difference, we first note that contrary to most previous works, the chains only contain a low number of rings. Consequently, no additional contribution to the elastic modulus is expected from the sliding-ring motion (i.e., we do not expect sliding elasticity). Second, as already mentioned, most of the chains contain a very low amount of ring cross-links. Therefore, when these rings can slide, the length of the trapped segments starts fluctuating, and it is expected that some of these network strands rapidly act as chain extenders for another network strand (Figure 6a), not participating to the sample elasticity anymore. As illustrated in Figure 6a, if we neglect the role of entanglements, then the length of network strands that are relaxed should progressively increase with the sliding of the chains through the ring cross-links. Consequently, with time, larger and larger fractions of the slide-ring network should be able to renew their configuration, leading to a progressive decrease of the storage modulus, toward the full relaxation of the gel. However, this is not observed: even if the cross-linking rings can slide, a remaining elasticity is observed at a long time. Based on the results found with the fixed-ring gel, we attribute this remaining elasticity to the presence of entanglements, which are unable to relax even if the ring cross-links can slide along the chains. Indeed, the disentanglement of a network strand trapped between two ring cross-links requires one of the ring cross-links to slide to the other side of the entanglement, dragging with it the whole part of the network, which is attached to the other side of the double ring. Depending on the cross-linking density, this process is either impossible or, if the network strand is located close to the dangling ends (Figure 6b,c), very slow.

To quantify the viscoelastic properties of the slide-ring gels, as a first estimate, we start from the fact that the density of entanglements is larger than the density of ring cross-links. Therefore, one can reasonably consider that each free-ring cross-link is able to slide at least a distance equal to the chain length between two entanglements, thus allowing the entanglement segments of mass M_e to relax (Figure 6b). Consequently, contrary to the fixed-ring gels (Figure 4a), the free-ring cross-links should not bring extra elasticity to the networks at a long time, and the corresponding relaxation modulus becomes

$$G(t) = G_{\text{Rouse}}(t) + G_N^0 \varphi_{\text{fixed ring}}(t)\phi_{\text{tube}}(t) \quad (5)$$

The storage and loss moduli predicted with eq 5 are shown in Figure 3b (dashed curves). The low-frequency elastic modulus found experimentally is much lower than the one predicted by assuming that the network relaxation is limited to the length scale of an entanglement segment. Thus, this result indicates that some entanglements located between two ring cross-links can also relax.

As shown in Figure 5a, the probability of a ring cross-link to be attached to a chain with only 1 or 2 ring cross-links is large. Consequently, as illustrated in Figure 6b,c, if such ring cross-links are located close to chain extremities, then the latter should be able to relax and disentangle via a contour length fluctuation (CLF) process involving the motion of the sparsely cross-linked chain. While this relaxation process starts from the chain extremities, it may propagate toward deeper segments, depending on the complexity of the pendant chains attached via the ring cross-links. In order to estimate the importance of this mechanism, we assume here that the CLF process of the PEO chains can take place as long as it implies the sliding of 1 (the outer one) ring cross-link through entanglements and stops as soon as it requires the sliding of two or more ring cross-links. It must be noted that this assumption is an approximation since in reality, we expect the CLF of some chain ends to stop at the first ring cross-link (if the latter is attached to a very complex architecture), while the CLFs of other chain ends could involve 2 or more cross-links (if they are attached to chains with one ring cross-link). The theoretical storage and loss moduli obtained with this assumption are shown in Figure 3b (continuous curves). We see that allowing the chain extremities to fluctuate over this longer distance leads to a much better description of the experimental data. In particular, the low-frequency elastic plateau is found to be much lower than that without accounting for this CLF process. This large influence of the CLF process is again attributed to the small number of rings per chain. At lower frequencies, the experimental low-frequency plateau continues to decrease, below the plateau predicted by considering CLFs involving the motion of one ring cross-link. This is most probably due to possible relaxation of even deeper segments by the same process but with a larger delay.

From this analysis, starting from the investigation of the viscoelastic properties of linear polyrotaxane, then of fixed-ring gels, and finally of free-ring gels without changing any other parameters and network connectivity, we conclude that the viscoelastic properties of the free-ring and fixed-ring gels originate from both the presence of entanglements between the network strands and the possible mobility of the cross-links. This mobility leads to the formation of longer network strands between the cross-linked rings, which may consist of several linear polyrotaxane strands. This, in turn, increases the mesh size of the free-ring gel. Without entanglements, this process should lead to the formation of longer strands. However, as our system is entangled, the ring mobility is limited to the entanglement strands since the motion of ring

https://doi.org/10.1021/acs.chemmater.4c01235
Chem. Mater. XXXX, XXX, XXX−XXX

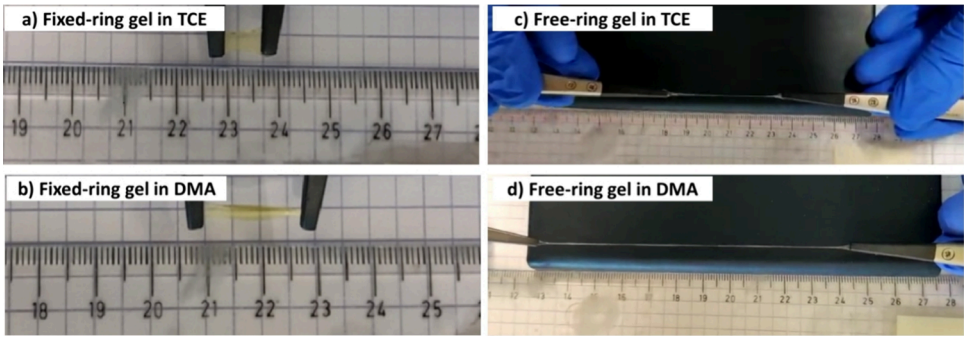

Figure 7. Maximum stretch state of the fixed-ring gels swollen in (a) TCE and (b) DMA and of the free-ring gels swollen in (c) TCE and (d) DMA.

cross-links cannot lead, a priori, to the loss of entanglements. Nevertheless, due to the low number of ring cross-links per chain, our results suggest that some entanglements can relax close to the chain extremities via a CLF relaxation process involving the sliding of the ring cross-links (together with the pendant chain) through the entanglements. The substantial decrease in elasticity after demetalation is thus attributed to the combined effect of ring mobility and loss of entanglements.

Stretchability of the Slide-Ring Gels. The stretchability of SRGs is an important property of this class of material since the pulley effect linked to the mobile junctions is expected to largely enhance the sample extensibility. Since the low amount of the samples did not allow us to characterize their mechanical properties in a tensile machine, we have checked their stretchability by a qualitative method, similarly to other researchers.[26,45] It is obvious that with such a method, the elongation rate is not controlled, but the difference between the sample behaviors was large enough that it could not be attributed to possible variations of the elongation rate. Figure 7 shows the stretchability of the four gels (Movies S1−S4). The stretchability was estimated by considering the length increase divided by the initial length:

$$\text{stretchability} = \frac{\text{final length before rupture} - \text{initial length}}{\text{initial length}} \times 100 = \frac{\Delta L}{L_0} \times 100 \quad (6)$$

Both fixed- and free-ring gels swollen in DMA or in TCE have been stretched by tweezers until their rupture is reached. The initial length of fixed-ring gels was 0.3 cm, while the length of the free-ring gels was fixed at 0.2 cm. Figure 7 shows the elongated gels just before the free-ring gels break and before the fixed-ring gels slip out of the tweezers, in both solvents. As expected, free-ring gels show a larger stretchability than the fixed ones because of the pulley effect of movable cross-links. It is also observed that the gels swollen in DMA show a higher stretchability. This can be attributed to the fact that there is no secondary interaction in these samples, and the pully effect is more efficient. Based on eq 6, the stretchability values of the fixed-ring gels are found to be almost equal to 167 and 500% in TCE and DMA, respectively, which are relatively low. This amount becomes much larger if the rings are free to move. In such a case, stretchability values of 3200 and 5500% are found in TCE and DMA, respectively. These values are higher than the best reported number (2500%) for a slide-ring gel based on naphthalene-containing molecular tubes, which had moreover a very low plateau modulus of 100 Pa.[45] The most stretchable SRG based on α-CD and PEO, developed through decreasing the average ring number on each strand, was able to stretch up to 1600% through tensile tests.[17] We attribute this ultra-stretchability to the large pulley effect obtained after removing Pd ions. This effect is more effective in our slide-ring gels because of the smaller number of rings that leads to a larger sliding distance for the free rings. This in turn leads to the formation of long oriented strands between ring cross-links and to an increase in the effective molecular weight between two cross-links, as proposed by other researchers based on experimental results[18] and simulation.[19]

CONCLUSIONS

In this work, we study the properties of palladium-based slide-ring gels obtained by a polyrotaxane approach. The introduction of metal−ligand complexes into the network provides a means to regulate the ring mobility by either preserving or eliminating the metal−ligand interactions between the ring and the thread, leading to a fixed-ring gel or a free-ring gel, respectively. The viscoelastic data of these gels demonstrate that the free-ring gels are softer and more resistant against shear rupture compared with the fixed-ring gels. The free-ring ring gels are also extremely stretchable, reaching extensibility up to 5500% by hand stretching, which is higher than other slide-ring gels reported and is explained by the very low density of ring cross-links favoring the efficient pulley effect and a long sliding distance. The influence of the solvent polarity was also investigated. The results reveal that the gel relaxation is delayed in a nonpolar solvent compared to a polar solvent, while both gels display a similar elastic modulus. Moreover, gels in polar solvents are more stretchable. These results are explained by the formation of hydrogen bonds between the polyrotaxane chains in the nonpolar solvent, which retard the relaxation and hamper the ring sliding.

To analyze the viscoelastic properties of these gels in detail, we developed a tube-based model that allowed us to quantify the density and average molar mass between two effective ring cross-links and to determine the fraction of dangling ends. This analysis revealed that the dynamics of slide-ring gels are influenced by two factors: (1) the sliding of the cross-links, which increases the effective mesh size of the networks with time, leading to a gradual decrease of the storage modulus, and (2) the presence of entanglements between the network strands, which restricts the sliding of the cross-links and gives rise to a remaining elasticity at a long time. Moreover, due to

https://doi.org/10.1021/acs.chemmater.4c01235
Chem. Mater. XXXX, XXX, XXX−XXX

the low number of ring cross-links per chain, our results suggest that some entanglements can relax near the chain extremities through a CLF process involving the diffusion of the outer-ring cross-links through the entanglements. The substantial decrease in elasticity and softness of the slide-ring gels after demetalation thus originates from the combined effect of cross-link mobility and loss of entanglements.

In conclusion, the metal−ligand-based SRG developed here not only allows the control of the ring density but also offers the possibility to control the ring mobility, from fixed rings to mobile rings, without changing other parameters of the system. The study of this system dynamics results in a clear picture of the peculiar viscoelastic behavior of SRGs for the first time, both experimentally and theoretically. This understanding is a crucial interconnection between the design of materials of this class and targeted final properties.

■ ASSOCIATED CONTENT

Supporting Information

The Supporting Information is available free of charge at https://pubs.acs.org/doi/10.1021/acs.chemmater.4c01235.

Experimental details, details on synthesis of polyrotaxane and gels and their characterization, and additional rheology data (PDF)

Videos of SRG stretching (ZIP)

■ AUTHOR INFORMATION

Corresponding Authors

Charles-André Fustin − *Bio and Soft Matter Division, Institute of Condensed Matter and Nanosciences, Université catholique de Louvain, Louvain-la-Neuve 1348, Belgium;* orcid.org/0000-0002-3021-5438; Email: charles-andre.fustin@uclouvain.be

Evelyne van Ruymbeke − *Bio and Soft Matter Division, Institute of Condensed Matter and Nanosciences, Université catholique de Louvain, Louvain-la-Neuve 1348, Belgium;* orcid.org/0000-0001-7633-0194; Email: evelyne.vanruymbeke@uclouvain.be

Authors

Sina Ghiassinejad − *Bio and Soft Matter Division, Institute of Condensed Matter and Nanosciences, Université catholique de Louvain, Louvain-la-Neuve 1348, Belgium*

Atul Kumar Sharma − *Bio and Soft Matter Division, Institute of Condensed Matter and Nanosciences, Université catholique de Louvain, Louvain-la-Neuve 1348, Belgium*

Complete contact information is available at: https://pubs.acs.org/10.1021/acs.chemmater.4c01235

Author Contributions

[+]S.G. and A.K.S. contributed equally to this work.

Notes

The authors declare no competing financial interest.

■ ACKNOWLEDGMENTS

E.v.R. is a Senior Research Associate of the FRS-FNRS. C.-A.F. and E.v.R. thank the Excellence of Science (EOS 40007519) program from the FWO and FRS-FNRS for financial support.

■ REFERENCES

(1) Lee, K. Y.; Mooney, D. J. Hydrogels for Tissue Engineering. *Chem. Rev.* **2001**, *101* (7), 1869−1880.

(2) Yang, C.; Suo, Z. Hydrogel Ionotronics. *Nat. Rev. Mater.* **2018**, *3* (6), 125−142.

(3) Le, X.; Lu, W.; Zhang, J.; Chen, T. Recent Progress in Biomimetic Anisotropic Hydrogel Actuators. *Adv. Sci.* **2019**, *6* (5), 1801584.

(4) Wu, B.; Lu, H.; Le, X.; Lu, W.; Zhang, J.; Théato, P.; Chen, T. Recent Progress in the Shape Deformation of Polymeric Hydrogels from Memory to Actuation. *Chem. Sci.* **2021**, *12* (19), 6472−6487.

(5) Qiu, Y.; Park, K. Environment-Sensitive Hydrogels for Drug Delivery. *Adv. Drug Delivery Rev.* **2001**, *53* (3), 321−339.

(6) Okumura, Y.; Ito, K. The Polyrotaxane Gel: A Topological Gel by Figure-of-Eight Cross-Links. *Adv. Mater.* **2001**, *13* (7), 485−487.

(7) Ito, K. Novel Cross-Linking Concept of Polymer Network: Synthesis, Structure, and Properties of Slide-Ring Gels with Freely Movable Junctions. *Polym. J.* **2007**, *39* (6), 489−499.

(8) Hart, L. F.; Hertzog, J. E.; Rauscher, P. M.; Rawe, B. W.; Tranquilli, M. M.; Rowan, S. J. Material Properties and Applications of Mechanically Interlocked Polymers. *Nat. Rev. Mater.* **2021**, *6*, 508−530.

(9) Ito, K. Novel Entropic Elasticity of Polymeric Materials: Why Is Slide-Ring Gel so Soft. *Polym. J.* **2012**, *44* (1), 38−41.

(10) Du, R.; Xu, Z.; Zhu, C.; Jiang, Y.; Yan, H.; Wu, H. C.; Vardoulis, O.; Cai, Y.; Zhu, X.; Bao, Z.; Zhang, Q.; Jia, X. A Highly Stretchable and Self-Healing Supramolecular Elastomer Based on Sliding Crosslinks and Hydrogen Bonds. *Adv. Funct. Mater.* **2020**, *30* (7), 1907139.

(11) Ikura, R.; Park, J.; Osaki, M.; Yamaguchi, H.; Harada, A.; Takashima, Y. Design of Self-Healing and Self-Restoring Materials Utilizing Reversible and Movable Crosslinks. *NPG Asia Mater.* **2022**, *14*, 10.

(12) Yi, M. B.; Lee, T. H.; Han, G. Y.; Kim, H.; Kim, H. J.; Kim, Y.; Ryou, H. S.; Jin, D. U. Movable Cross-Linking in Adhesives: Superior Stretching and Adhesion Properties via a Supramolecular Sliding Effect. *ACS Appl. Polym. Mater.* **2021**, *3* (5), 2678−2686.

(13) Bin Imran, A.; Esaki, K.; Gotoh, H.; Seki, T.; Ito, K.; Sakai, Y.; Takeoka, Y. Extremely Stretchable Thermosensitive Hydrogels by Introducing Slide-Ring Polyrotaxane Cross-Linkers and Ionic Groups into the Polymer Network. *Nat. Commun.* **2014**, *5*, 5124.

(14) Chen, L.; Sheng, X.; Li, G.; Huang, F. Chem Soc Rev Mechanically Interlocked Polymers Based on Rotaxanes. *Chem. Soc. Rev.* **2022**, *51*, 7046−7065.

(15) Harada, A.; Hashidzume, A.; Yamaguchi, H.; Takashima, Y. Polymeric Rotaxanes. *Chem. Rev.* **2009**, *109* (11), 5974−6023.

(16) Kato, K.; Okabe, Y.; Okazumi, Y.; Ito, K. A Significant Impact of Host-Guest Stoichiometry on the Extensibility of Polyrotaxane Gels. *Chem. Commun.* **2015**, *51* (90), 16180−16183.

(17) Jiang, L.; Liu, C.; Mayumi, K.; Kato, K.; Yokoyama, H.; Ito, K. Highly Stretchable and Instantly Recoverable Slide-Ring Gels Consisting of Enzymatically Synthesized Polyrotaxane with Low Host Coverage. *Chem. Mater.* **2018**, *30* (15), 5013−5019.

(18) Liu, C.; Morimoto, N.; Jiang, L.; Kawahara, S.; Noritomi, T.; Yokoyama, H.; Mayumi, K.; Ito, K. Tough Hydrogels with Rapid Self-Reinforcement. *Science* **2021**, *372* (6546), 1078−1081.

(19) Gavrilov, A. A.; Potemkin, I. I. Adaptive Structure of Gels and Microgels with Sliding Cross-Links: Enhanced Softness. *Stretchability and Permeability. Soft Matter* **2018**, *14* (24), 5098−5105.

(20) Kato, K.; Karube, K.; Nakamura, N.; Ito, K. The Effect of Ring Size on the Mechanical Relaxation Dynamics of Polyrotaxane Gels. *Polym. Chem.* **2015**, *6* (12), 2241−2248.

(21) Jin, C.; Park, J.; Shirakawa, H.; Osaki, M.; Ikemoto, Y.; Yamaguchi, H.; Takahashi, H.; Ohashi, Y.; Harada, A.; Matsuba, G.; Takashima, Y. Synergetic Improvement in the Mechanical Properties of Polyurethanes with Movable Crosslinking and Hydrogen Bonds. *Soft Matter* **2022**, *18* (27), 5027−5036.

(22) Jin, J. N.; Yang, X. R.; Wang, Y. F.; Zhao, L. M.; Yang, L. P.; Huang, L.; Jiang, W. Mechanical Training Enabled Reinforcement of Polyrotaxane-Containing Hydrogel. *Angew. Chem., Int. Ed.* **2023**, *62* (8), No. e202218313.

(23) Sawada, J.; Aoki, D.; Uchida, S.; Otsuka, H.; Takata, T. Synthesis of Vinylic Macromolecular Rotaxane Cross-Linkers Endowing Network Polymers with Toughness. *ACS Macro Lett.* **2015**, *4* (5), 598−601.
(24) Takata, T. Switchable Polymer Materials Controlled by Rotaxane Macromolecular Switches. *ACS Cent. Sci.* **2020**, *6* (2), 129−143.
(25) Sawada, J.; Aoki, D.; Otsuka, H.; Takata, T. A Guiding Principle for Strengthening Crosslinked Polymers: Synthesis and Application of Mobility-Controlling Rotaxane Crosslinkers. *Angew. Chem., Int. Ed.* **2019**, *58* (9), 2765−2768.
(26) Yamamoto, K.; Nameki, R.; Sogawa, H.; Takata, T. Macrocyclic Dinuclear Palladium Complex as a Novel Doubly Threaded [3] Rotaxane Scaffold and Its Application as a Rotaxane Cross-Linker. *Angew. Chem., Int. Ed.* **2020**, *59* (41), 18023−18028.
(27) Hart, L. F.; Lenart, W. R.; Hertzog, J. E.; Oh, J.; Turner, W. R.; Dennis, J. M.; Rowan, S. J. Doubly Threaded Slide-Ring Polycatenane Networks. *J. Am. Chem. Soc.* **2023**, *145* (22), 12315−12323.
(28) Sharma, A. K.; Malineni, J.; Box, S.; Ghiassinejad, S.; Van Ruymbeke, E.; Fustin, C.-A. Synthetic Platform for Mono-Functionalised Tridentate Macrocycles as Key Precursors of Mechanically-Linked Macromolecular Systems. *Org. Chem. Front.* **2021**, *8*, 2383−2392.
(29) Ogawa, M.; Kawasaki, A.; Koyama, Y.; Takata, T. Synthesis and Properties of a Polyrotaxane Network Prepared from a Pd-Templated Bis-Macrocycle as a Topological Cross-Linker. *Polym. J.* **2011**, *43* (11), 909−915.
(30) Ogawa, M.; Sogawa, H.; Koyama, Y.; Takata, T. Synthesis of Rotaxane Cross-Linked Polymers Derived from Vinyl Monomers Using a Metal-Containing Supramolecular Cross-Linker. *Polym. J.* **2015**, *47* (8), 580−584.
(31) Kato, K.; Ito, K. Dynamic Transition between Rubber and Sliding States Attributed to Slidable Cross-Links. *Soft Matter* **2011**, *7* (19), 8737−8740.
(32) Kato, K.; Yasuda, T.; Ito, K. Viscoelastic Properties of Slide-Ring Gels Reflecting Sliding Dynamics of Partial Chains and Entropy of Ring Components. *Macromolecules* **2013**, *46* (1), 310−316.
(33) Fuller, A.-M.; Leigh, D. A.; Lusby, P. J.; Oswald, I. D. H.; Parsons, S.; Walker, D. B. A 3D Interlocked Structure from a 2D Template: Structural Requirements for the Assembly of a Square-Planar Metal-Coordinated [2] Rotaxane. *Angew. Chemie Int. Ed.* **2004**, *43* (30), 3914−3918.
(34) Fuller, A. M. L.; Leigh, D. A.; Lusby, P. J.; Slawin, A. M. Z.; Walker, D. B. Selecting Topology and Connectivity through Metal-Directed Macrocyclization Reactions: A Square Planar Palladium [2]Catenate and Two Noninterlocked Isomers. *J. Am. Chem. Soc.* **2005**, *127* (36), 12612−12619.
(35) Fuller, A. L.; Leigh, D. A.; Lusby, P. J. One Template, Multiple Rings: Controlled Iterative Addition of Macrocycles onto a Single Binding Site Rotaxane Thread. *Angew. Chem., Int. Ed.* **2007**, *46* (26), 5015−5019.
(36) Ahamed, B. N.; Duchêne, R.; Robeyns, K.; Fustin, C. A. Catenane-Based Mechanically-Linked Block Copolymers. *Chem. Commun.* **2016**, *52* (10), 2149−2152.
(37) Fleury, G.; Schlatter, G.; Brochon, C.; Hadziioannou, G. From High Molecular Weight Precursor Polyrotaxanes to Supramolecular Sliding Networks. The "Sliding Gels. *Polymer* **2005**, *46* (19), 8494−8501.
(38) Fleury, G.; Schlatter, G.; Brochon, C.; Hadziioannou, G. Unveiling the Sliding Motion in Topological Networks: Influence of the Swelling Solvent on the Relaxation Dynamics. *Adv. Mater.* **2006**, *18* (21), 2847−2851.
(39) Yang, X.; Cheng, L.; Zhang, Z.; Zhao, J.; Bai, R.; Guo, Z.; Yu, W.; Yan, X. Amplification of Integrated Microscopic Motions of High-Density [2]Rotaxanes in Mechanically Interlocked Networks. *Nat. Commun.* **2022**, *13*, 6654.
(40) Shi, C. Y.; Zhang, Q.; Yu, C. Y.; Rao, S. J.; Yang, S.; Tian, H.; Qu, D. H. An Ultrastrong and Highly Stretchable Polyurethane Elastomer Enabled by a Zipper-Like Ring-Sliding Effect. *Adv. Mater.* **2020**, *32* (23), 2000345.
(41) Van Ruymbeke, E.; Keunings, R.; Bailly, C. Prediction of Linear Viscoelastic Properties for Polydisperse Mixtures of Entangled Star and Linear Polymers: Modified Tube-Based Model and Comparison with Experimental Results. *J. Nonnewton. Fluid Mech.* **2005**, *128* (1), 7−22.
(42) Van Ruymbeke, E.; Bailly, C.; Keunings, R.; Vlassopoulos, D. A General Methodology to Predict the Linear Rheology of Branched Polymers. *Macromolecules* **2006**, *39* (18), 6248−6259.
(43) Goldansaz, H.; Voleppe, Q.; Piogé, S.; Fustin, C. A.; Gohy, J. F.; Brassinne, J.; Auhl, D.; Van Ruymbeke, E. Controlling the Melt Rheology of Linear Entangled Metallo-Supramolecular Polymers. *Soft Matter* **2015**, *11* (4), 762−774.
(44) Hawke, L. G. D.; Ahmadi, M.; Goldansaz, H.; Van Ruymbeke, E. Viscoelastic Properties of Linear Associating Poly(n-Butyl Acrylate) Chains. *J. Rheol.* **2016**, *60* (2), 297−310.
(45) Ke, H.; Yang, L. P.; Xie, M.; Chen, Z.; Yao, H.; Jiang, W. Shear-Induced Assembly of a Transient yet Highly Stretchable Hydrogel Based on Pseudopolyrotaxanes. *Nat. Chem.* **2019**, *11* (5), 470−477.

https://doi.org/10.1021/acs.chemmater.4c01235
Chem. Mater. XXXX, XXX, XXX−XXX